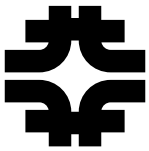

Fermi National Accelerator Laboratory

FERMILAB-Pub-95/138-E
E781

A Method to Evaluate Mirrors for Cherenkov Counters

Linda Stutte, Jurgen Engelfried and James Kilmer

Fermi National Accelerator Laboratory
P.O. Box 500, Batavia, Illinois 60510

June 1995

Submitted to *Nuclear Instruments and Methods*

Operated by Universities Research Association Inc. under Contract No. DE-AC02-76CHO3000 with the United States Department of Energy

Disclaimer

A Method to Evaluate Mirrors for Cherenkov Counters

Linda Stutte, Jürgen Engelfried and James Kilmer
*Fermi National Accelerator Laboratory**
P.O. Box 500, Batavia, IL 60510

Abstract

A method is evaluated for measuring mirrors to be used in a Ring Imaging Cherenkov Counter. It was first used to evaluate astronomical quality mirrors, but has been found to be applicable for the lower surface quality of Cherenkov mirrors.

1 Introduction

The authors are building a Ring Imaging Cherenkov Counter to identify particle types in charmed baryon decays in Fermilab experiment E781 (SELEX) [1]. The Cherenkov light will be focussed by an array of 16 hexagonally-shaped spherical mirrors (20 m radius of curvature) onto a photocathode that consists of 2848 phototubes of 15 mm diameter. A design goal for the mirrors is that they do not contribute significantly to the error on reconstructed Cherenkov ring radii. This translates to an RMS width of about 5 cm ($\frac{1}{4}$ %) for both the variation in radius of curvature across a single mirror as well as the variation from mirror to mirror of the average radius of curvature. This criterion is much below that needed for astronomical mirrors.

Initial efforts to determine mirror quality by scanning a laser beam over the mirror surface were compromised by variable air currents over the necessarily long measurement times. The method described in this paper, used by amateur telescope makers [2] to evaluate their mirrors, has the advantage of being an integral measurement and also has the required precision.

After describing the method and experimental setup, sample data from three mirrors from other Fermilab Cherenkov detectors are presented. The data reduction method is described and a Monte Carlo simulation to benchmark the image processing software is discussed.

2 The Ronchi Method

Figure 1 shows the Ronchi method. A light source is placed at approximately the center of curvature of the mirror to be studied, at distance S from the mirror, as shown in the figure. A narrow slit is placed in the path of the light to form a line source. The reflected light

*Work supported by the U.S. Department of Energy under contract NO. DE–AC02–76CHO3000

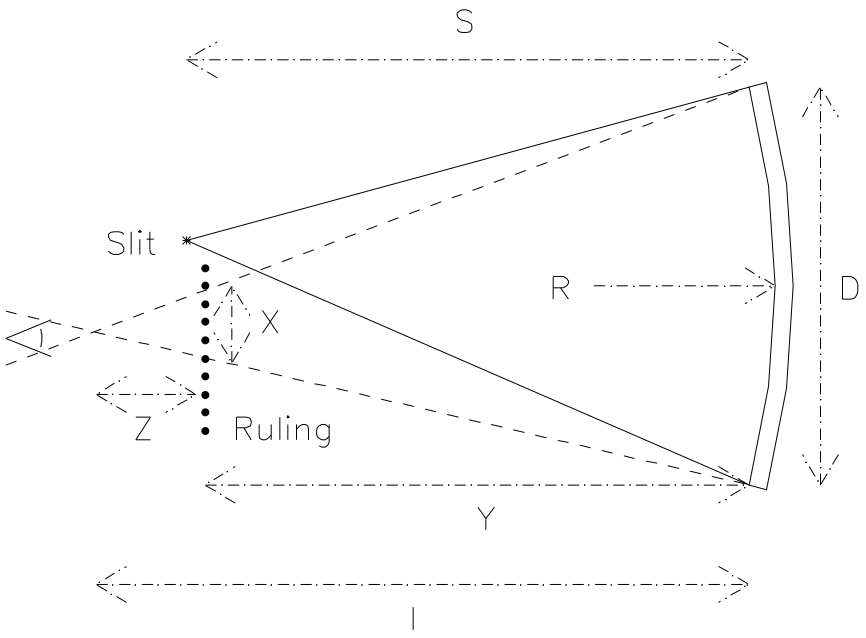

Figure 1: Schematic Diagram of the Ronchi Measurements

forms an image at a distance I from the mirror. A finely ruled grating (the Ronchi Ruling) is placed in the path of the reflected light at a known distance Y from the mirror. This grating has lines of equal opaque and clear widths running in the same direction as the slit, of spacing G. One views the mirror through this grating, either with the eye, or, in this case, with a camera. A given orientation of the grating is only sensitive to the radius of curvature perpendicular to the grating direction. In general, several different orientations should be measured to get a complete picture of any given mirror.

If the Ruling is placed exactly at the image point of the mirror either a uniformly bright or uniformly dark picture of the mirror is seen. As the Ruling is moved away from the image point alternate dark and light bands appear across the picture of the mirror. Quantitatively, by similar triangles

$$\frac{X}{Z} = \frac{D}{I} \tag{1}$$

where X is the portion of the Ruling which intercepts the returned light, Z is the distance of the Ruling from the image point and D is the diameter of the mirror. N_{bands}, the number of lines observed across the picture of the mirror, is just

$$N_{\mathrm{bands}} = \frac{X}{G} \tag{2}$$

With the relation

$$I = Z + Y \tag{3}$$

one obtains a formula for the distance of the image from the mirror which is based on observable quantities:

$$I = \frac{D * Y}{D \mp G * N_{\text{bands}}} \tag{4}$$

The minus sign in the above equation is valid if the Ruling is between the image point and the mirror, and the plus sign is valid if the Ruling is between the image point and the camera.

This result can be combined with the measured source distance in the mirror equation:

$$\frac{1}{S} + \frac{1}{I} = \frac{2}{R} \tag{5}$$

to compute the mirror radius of curvature R.

Additionally, for a mirror with variations in the radius of curvature across its surface, the above technique can also be used to measure that variation. Instead of looking at the number of bands across the whole mirror and computing a global image point, one uses the local spacing between individual bands to compute a local image point. In the equations above, N_{bands} becomes 1, and D, the diameter of the mirror, is replaced by dB, the spacing between bands, as measured on the surface of the mirror. These individually determined image points (or, in practice, their corresponding radii of curvature) can be summed to determine the quality of a mirror. This local method gives accurate results as long as the variations in radius of curvature are small. Errors depend on the gradient and increase with the radial distance from the mirror center. A numeric example is described in a later section.

For mirrors with radius of curvature that are very large compared to the Ruling slit width ($\geq 10^5$) the light becomes parallel enough to observe Fraunhofer diffraction. This is a fundamental limitation in this method.

3 The Experimental Setup

Figure 2: Experimental Setup; a) Light Source and Ruling, b) Mirror in mount

Figures 2a and 2b show the actual apparatus used in these measurements. Figure 2a shows the light source consisting of a 500 W light bulb mounted in an aluminum housing with a fan on top for cooling. The slit which formed the line source was made out of two machined edges. It could be rotated to a variety of selected angles. Also shown at the left of the figure is the Ronchi Ruling mounted in a holder which accommodated vertical or horizontal orientations of the Ruling. (Additional holders were available for other angles.) As a compromise between diffraction effects and sensitivity, a Ruling of spacing 0.0508 cm/line was used throughout these measurements. The Ruling was placed on a long machined-surface table, which had a scale attached along its length for easy measurement of distances. The camera which viewed the mirror is visible at the back of the picture. Data were recorded onto VHS videocassettes using a standard VCR. In addition, output from a microphone was simultaneously recorded in order to note the placement of the Ruling. These images were subsequently 'frame- grabbed' using standard software available on an SGI-Indy[3]. Analysis of the data is described in a later section. Figure 2b shows a mirror in one of several mirror supports used for these measurements. The mirrors were typically located at a distance from the light source and the Ruling which was approximately their radius of curvature.

4 A Uniform Mirror

The first mirror [4] measured ('The Dichromatic Cherenkov Mirror') was used at Fermilab to measure particle fractions in the secondary charged particle beam produced to form a dichromatic neutrino beam [5]. It is 30.48 cm in diameter, with a 609.6 cm radius of curvature. It is a thick mirror, housed in a sturdy steel support. Because this mirror is of good uniformity, the number of bands observed across the mirror diameter as a function of distance can be used to determine a common radius of curvature for the entire mirror. Figure 3 shows a 'Ronchigram' taken of this mirror at about 10 cm distance of the Ruling from the image point. Some of the waviness of the lines is due to air currents. This is evident at the perimeter of the mirror. In fig. 4 the number of bands observed across the mirror is plotted versus the position of the Ruling. The points for which the Ruling is between the image and the camera are also entered on the figure with negative N_{bands}. A good straight line fit results, with the number of lines equal zero at a distance of 5 cm in this local co-ordinate system. Using this zero point, and extrapolating the data in the figure to the end of the table (at 30 cm on the figure), one can solve for both the unknown distance from the end of the table to the mirror and the radius of curvature of the mirror. One obtains a radius of curvature of 608.95 cm, which is within 0.1 % of the nominal radius.

5 A Mirror with two Regions of Different Radius

The second mirror measured ('The Beamline Cherenkov Mirror') came from one of the Fermilab Fixed Target Beamline Cherenkov counters [6]. It was about 1.27 cm thick (with a hollowed-out region for the beam near the center), 30.48 cm in diameter and had an average radius of curvature of approximately 520 cm. A notation saying 'bad spot near center' appeared on it's packaging. It had no stand - the mirror was placed against a chair for the

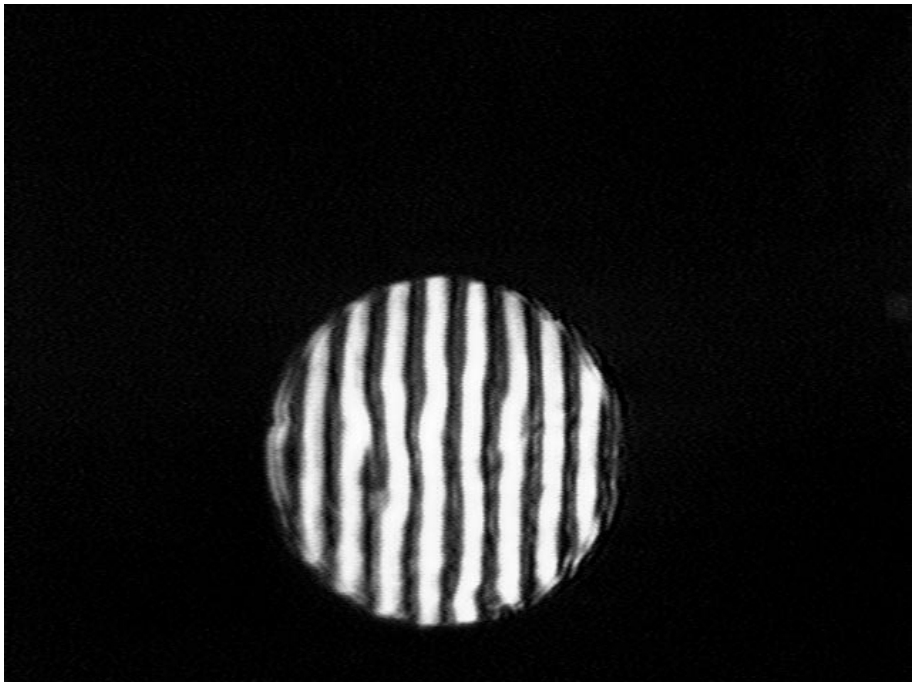

Figure 3: Ronchigram of the Dichromatic Cherenkov Mirror

measurement. A Ronchigram for this mirror with the Ruling close to the average image point of the outer region is shown in fig. 5. The different radius at the center of the mirror is clearly evident. The number of bands observed over a fixed distance on the image, extrapolated to the entire width of the mirror, is plotted in fig. 6 as a function of distance between the Ruling and the mirror, separately for both the inner and outer regions. The two lines intercept zero at a relative distance of approximately 36 cm, indicating that the radii of curvature are approximately 18 cm different for the two regions.

6 Testbeam Cherenkov Mirror

The third mirror measured was used in the RICH detector of Fermilab experiment E781T [7]. It was about 1 inch thick [8], also with a hollowed-out beam region, 50.6 cm in diameter and had a radius of curvature of about 20 m. Ronchigrams of it at a single distance, but at two different orientations of the Ruling are shown in fig. 7a and 7b. Some non-uniformities in the upper left quadrant are evident in the figures. Also seen is a 'halo' which appears at the left and right of the image in fig. 7a, and at the top and bottom of the image in fig. 7b, which is due to the previously mentioned Fraunhofer diffraction effect. This halo is also present but less evident in the Ronchigrams shown in figs. 3 and 5.

Due to the non-uniformity of this mirror, the global band-counting technique was not applicable. Instead the local band spacing as a function of position across the mirror surface was measured and a distribution of mirror radii of curvature was calculated. The analysis

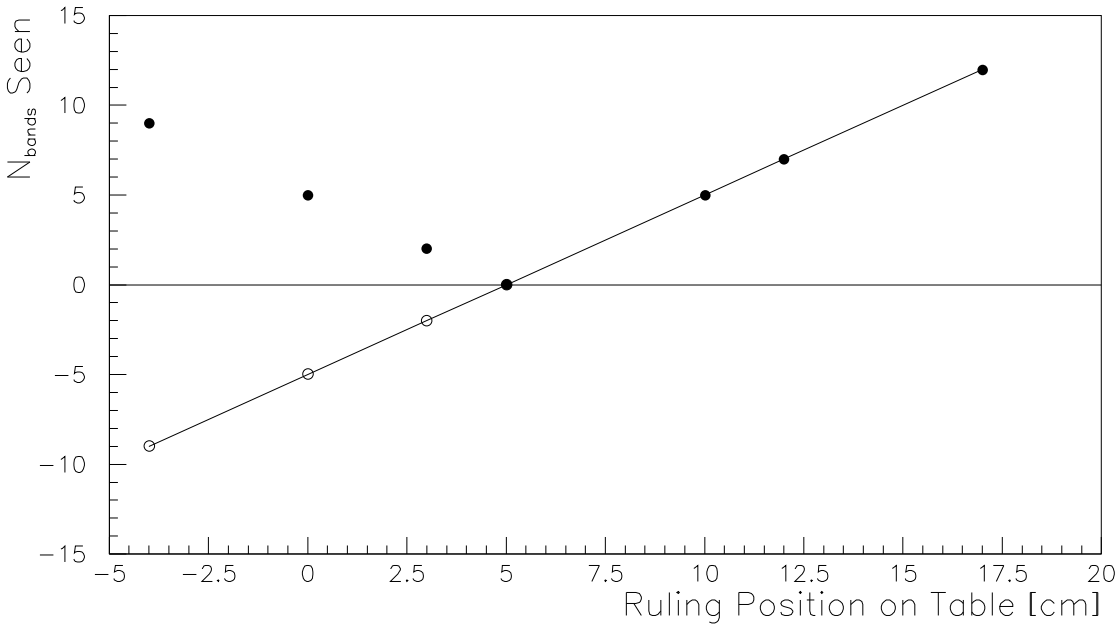

Figure 4: Number of Observed Bands versus Position of the Ruling for the Dichromatic Cherenkov Mirror

of this mirror is used as an example in the next section which describes the technique.

7 Data Reduction Method

The pictures in fig. 7 are postscript files of images which were 'frame-grabbed' from one of the videotapes. The product xv [9] was used to take an image (initially stored in .rgb format) and convert it into standard postscript. This program can convert images into many different formats. Another format (.pgm) was used to convert the image into an ascii greyscale pixel representation for image processing. This pixel representation was read into an array by a Fortran program written to process the images and is displayed as a 2-dimensional histogram using PAW [10] in the upper lefthand plot in fig. 8. The array is first scaled to an average intensity. Then the edges of the image are extracted in order to define the area of the plot which contains the Ronchigram. The algorithm used is to scan individual rows of the pixel array from each side to find the points at which the intensity exceeds a pre-selected threshold. These points are called the edges, and they are used to fit a circle which defines the extent of the image. The intensity of array elements within the boundaries of the image are then adjusted a final time to give approximately equal density of white and black areas on the picture. The array is smoothed over three bins perpendicular to the direction of the bands and summed over three bins parallel to the direction of the bands in order to get a more uniformly varying representation.

An algorithm is employed to search for bands in all the rows perpendicular to the direction

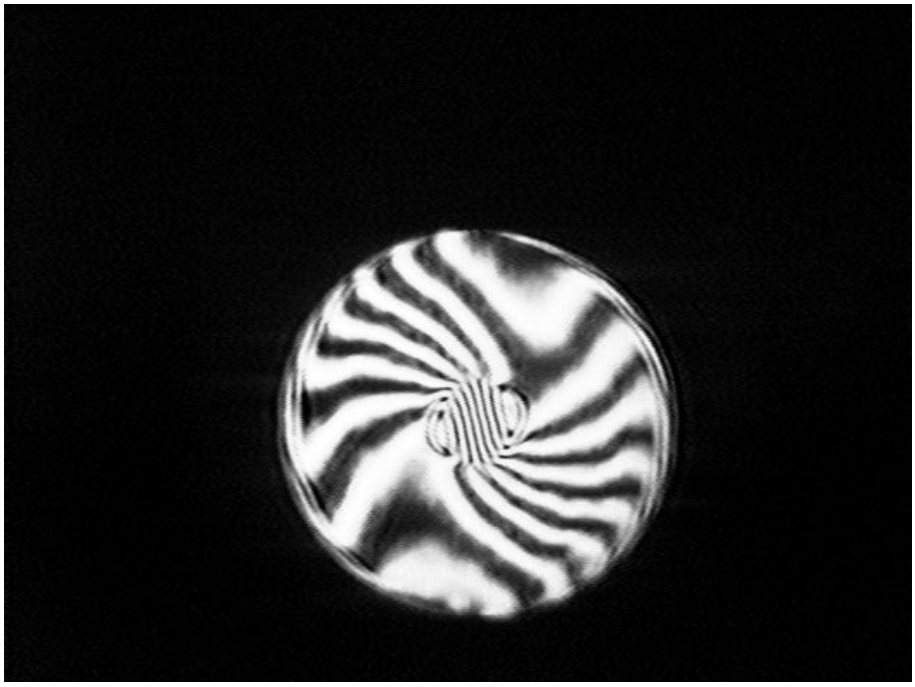

Figure 5: Ronchigram of the Beamline Cherenkov Mirror

of the Ruling, using threshold seeking techniques to locate the band peaks and the valleys between bands. A gaussian fit is performed to finalize each band location. Bands are linked together from row to row, so that even though a peak might be missed in a row or two, the band computation software can make up for this by using information from close-by 'linked' rows. It was also found that this linking method is needed to correctly process images in which the Ruling is at an angle other than 0 or 90 degrees. The results of the band search algorithm for this image are shown as the upper righthand plot in fig. 8, which can be compared to the postscript representation in fig. 7a. Finally, in each row, the distance between adjacent bands is computed and the formulas given previously are used to determine the variation in mirror radii, shown for this image in the lower righthand plot of fig. 8 and versus position on the mirror in the lower lefthand plot of fig. 8.

A known problem with this pattern recognition software is non-uniform illumination of the mirror by the light source, which can cause the intensity of sections of the image to drop below the pre-set threshold for band recognition. This can be compensated in part with a position dependent normalization. Another problem is caused by the Fraunhofer diffraction discussed earlier, which can wash out the variation between peaks and valleys, especially for some band spacings. This is just a fundamental limitation of this technique for which there is no known cure.

The Testbeam mirror was studied extensively. Data were taken at many distances, and the orientation of the Ruling was varied. The mirror was measured on several different days. From these systematic studies it was determined that the average radius of curvature was measured to about 5 cm accuracy, mainly limited by the care taken in measuring the

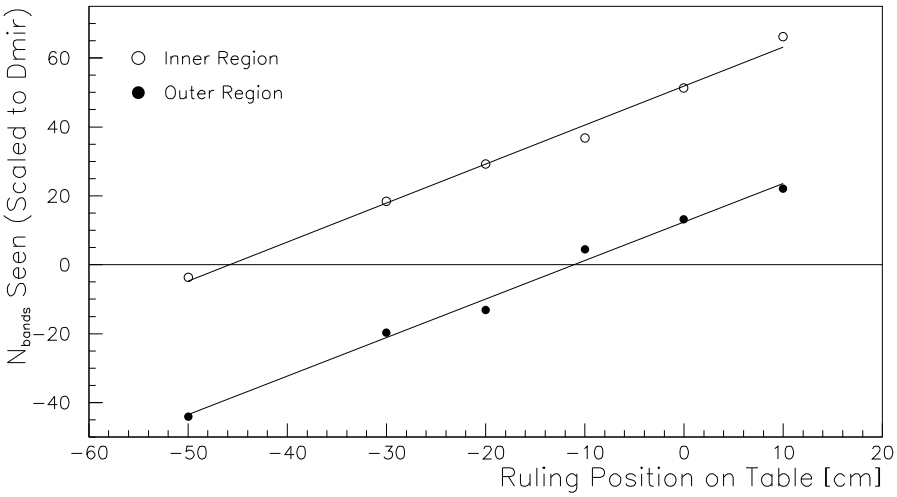

Figure 6: Number of Observed Bands versus Position of the Ruling for the Beamline Cherenkov Mirror

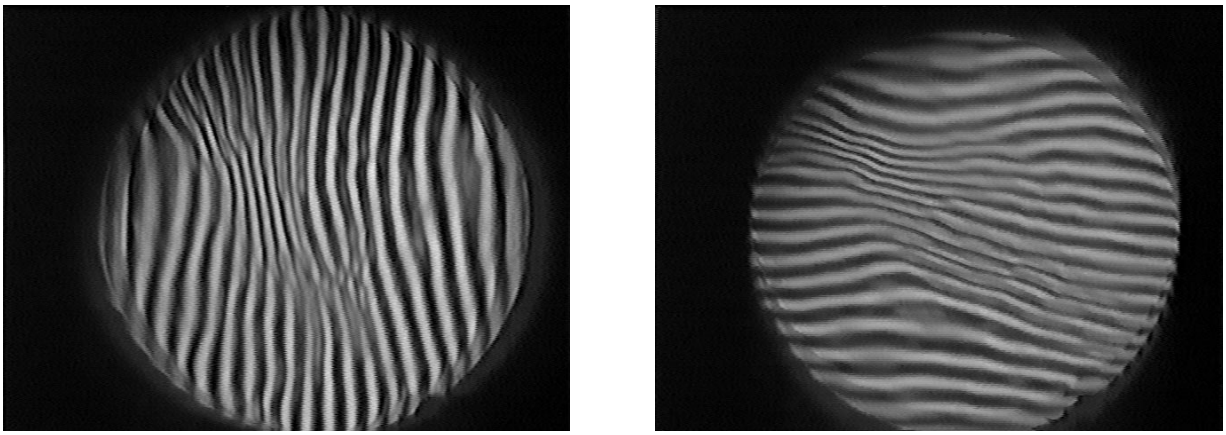

Figure 7: Ronchigrams of the Testbeam Mirror a) Vertical and b) Horizontal Orientations of the Ruling

various distances. The measurements of radius variation could be repeated to about 1 cm accuracy, mainly limited by the image processing software. The final RMS radius variation was consistent with the measured ring radius resolution from the testbeam data.

8 Monte Carlo Studies

In order to study what kinds of mirror distortions resulted in observable patterns, and primarily, to benchmark the image processing software, a series of Monte Carlo studies were

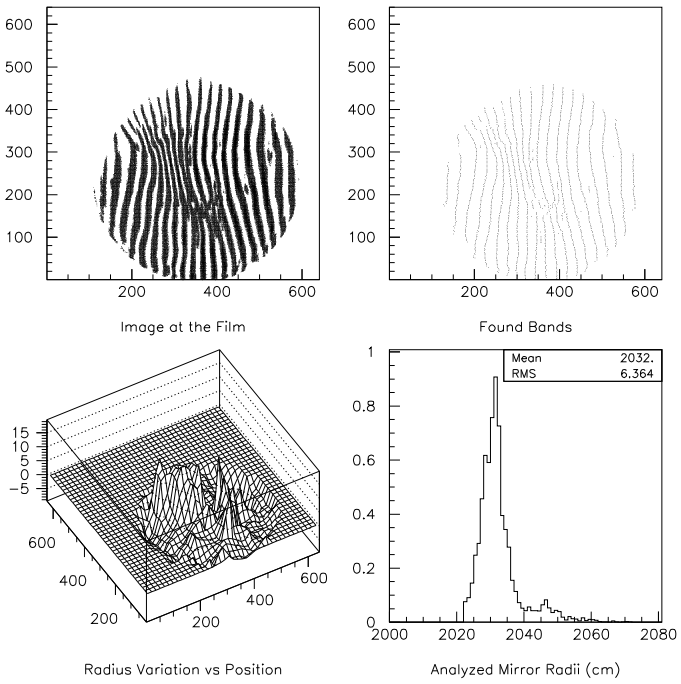

Figure 8: Data Reduction – ASCII Greyscale Representation, Threshold Seeking Algorithm Results, Analysis Results of the Testbeam Mirror

carried out. Rays were generated from a light source, propagated to a mirror, reflected from it and transmitted through a grating, a camera lens and finally recorded at the film location. The mirror was modelled as a 40 cm diameter surface of small (1 mm) pixels, each one of which had its own radius and center of curvature. Several separate mirror distortions were modelled.

Modelling a perfect mirror of radius 2000 cm, it was found that the image processing software reconstructs an average radius of 1999 cm with less than 1 cm RMS deviation from this average.

Another model studied consisted of a uniform mirror with a sizeable area with another radius of curvature ('the Bad Spot'). In fig. 9 the upper lefthand plot contains the generated Ronchigram. The upper righthand plot displays the distribution of generated radii. The two lower plots show the result of the analysis: the lefthand plot is the reconstructed radius vs position on the mirror surface and the righthand plot is the distribution of reconstructed radii. For this model there is good agreement between the generated and reconstructed radii, independent of the position of the bad spot upon the mirror surface.

A third model studied had a radius of curvature which varied linearly with radial position on the mirror surface. The magnitude of the variation could be selected, and it could have either sign. Figure 10 displays information about this model in the same format as fig. 9. The example shown in the figure has a larger radius of curvature than average near the center of the mirror, and a smaller radius of curvature than average near the edges of the mirror. Here

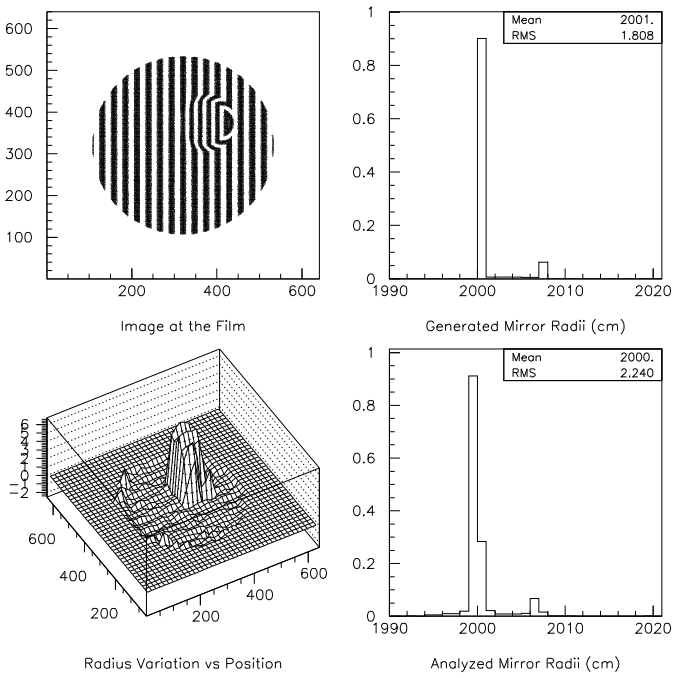

Figure 9: Monte Carlo Analysis – Bad Spot

the agreement between the generated and reconstrated radii is not as good as for the other models. The radii near the mirror edges (the smallest radii) are reconstructed at smaller than generated values. This can be attributed to the previously mentioned problem of large gradients across the mirror surface. This effect was studied extensively, varying several parameters including the sign and magnitude of the gradient and the relative position of the Ronchi Ruling and the mirror. It was found that the disagreement between the generated and the reconstructed RMS of the mirror radii distributions never exceeded a factor of two.

Additional models with mirror distortions which varied according to direction on the mirror surface were also studied and pointed out the importance of examining Ronchigrams at various orientations.

9 Conclusions

This paper presented an integral method for measuring mirrors to be used in a Ring Imaging Cherenkov Counter. This method, first used to evaluate astronomical quality mirrors, has been found to be applicable and gives quantitatively correct results for the lower surface quality (about $\frac{1}{4}$ %) found in Cherenkov mirrors. For mirrors with larger surface variations only qualitative results can be obtained. Measurements are now in progress using this method to evaluate the mirrors to be used in the SELEX RICH detector.

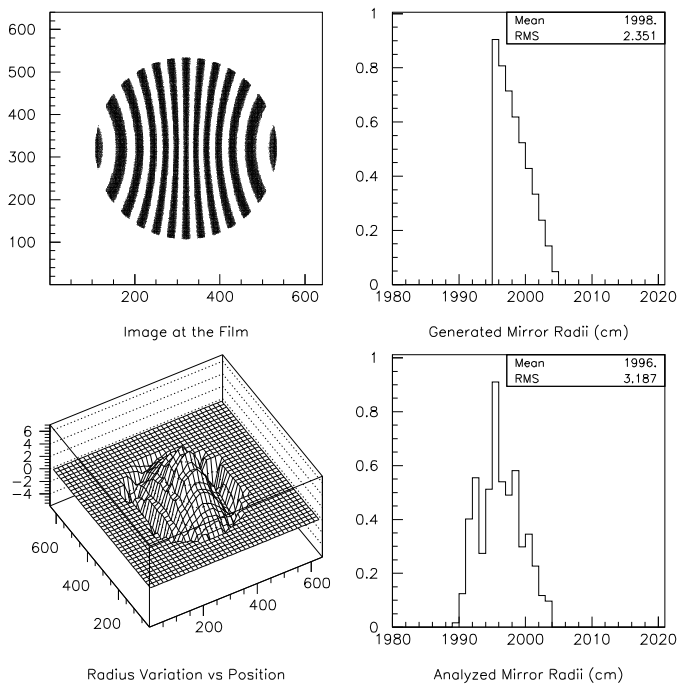

Figure 10: Monte Carlo Analysis – Linear Radial Variation

10 Acknowledgements

The authors wish to thank Joseph Lach for his suggestion to investigate this method and Edgar de Oliveira for his help with early measurements. We wish to thank the Fermilab Research Division Mechanical Department for their timely assistance in fabricating the hardware used in these measurements and both the Fermilab Research Division Electrical Department and Fermilab Visual Media Services for providing the video equipment.

References

[1] J. Russ, *Charm Baryon Physics – Present and Future*, proceedings of Workshop on the Future of High Sensitivity Charm Experiments: CHARM2000, Batavia, Ill., Jun 7-9, 1994, FERMILAB-CONF-94/190.

[2] A. G. Ingalls, ed., *Amateur Telescope Making*, Scientific American Inc (1981).

[3] Silicon Graphics Inc., Mountain View, CA.

[4] A. Bodek, et al, *Observation of Light Below Cherenkov Threshold in a Short Cherenkov Counter*, Zeit. fur Phys. C, **18**, 289 (1983).

[5] D. Edwards, S. Mori, S. Pruss, *350 Gev/c Dichromatic Neutrino Train*, FNAL TM–661 (1976).

[6] G. Koizumi, Private communication.

[7] M.P.Maia et al., *A Phototube RICH Detector*, Nucl. Instr. and Meth. A326 (1993) 496.

[8] K. B. Luk, Private communication.

[9] J. Bradley, University of Pennsylvania (1993).

[10] PAW, CERN Program Library entry Q121.